Experimental, analytical, and numerical study of transient elastic waves from a localized source in an aluminium strip

M. Mračko[a], V. Adámek[b,*], A. Berezovski[c,a], J. Kober[a], R. Kolman[a]

[a] *Institute of Thermomechanics, v.v.i., The Czech Academy of Sciences, Dolejškova 1402/5, 182 00 Praha 8, Czech Republic*
[b] *NTIS - New Technologies for the Information Society, Faculty of Applied Sciences, University of West Bohemia, Technická 8, 301 00 Pilsen, Czech Republic*
[c] *Department of Cybernetics, School of Science, Tallinn University of Technology, Akadeemia 21, 12618 Tallinn, Estonia*

Abstract

In the paper, two-dimensional wave propagation in an aluminium strip is examined experimentally, analytically, and numerically. Experimentally, the high-frequency pulse is generated by a piezoelectric transducer, and the velocity component normal to the strip edge is measured by the non-contact vibrometer system on the opposite side. The analytical method used for the investigation of two-dimensional in-plane waves propagated under plane stress conditions is based on the combination of Laplace and Fourier transforms. The main question is the suitability of numerical procedures to represent the transient wavefield observed in the experiment. In two-dimensional numerical solutions, explicit variants of the finite element and finite volume solvers are utilized. It is demonstrated that standard finite volume and finite element algorithms conform analytical results and the numerical results are in a good agreement with experiment for time observation including several wave reflections from upper and bottom boundaries. The experimental, analytical, and numerical results presented in this study can be used as a benchmark data for the investigation of transient waves in a two-dimensional

*Corresponding author
Email addresses: mracko@it.cas.cz (M. Mračko), vadamek@kme.zcu.cz (V. Adámek), Arkadi.Berezovski@cs.ioc.ee (A. Berezovski), kober@it.cas.cz (J. Kober), kolman@it.cas.cz (R. Kolman)

elastic medium to validate other numerical or semi-analytical methods.

Keywords: wave propagation, elastic strip, experimental measurement, finite element method, finite volume method, analytical solution, plane stress problem

---

1. Introduction

The simplest possible scheme of ultrasonic nondestructive testing (such as presented in Fig. 1) suggests that the signal issued by a transmitter is recorded by a receiver. The difference in the shape and phase between initial and reflected signals can be interpreted as the existence of a defect inside the specimen.

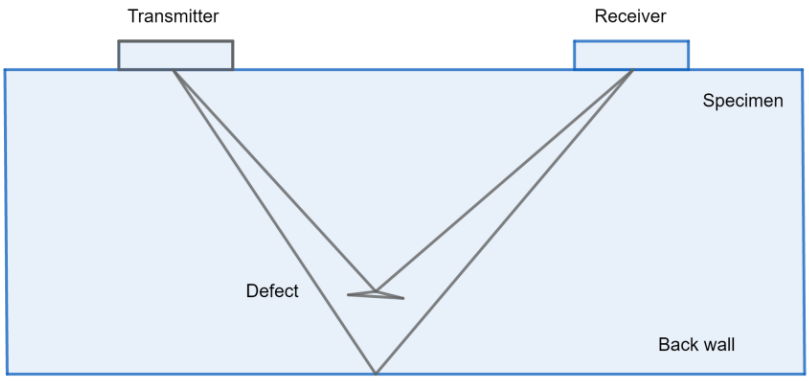

Figure 1: Transmitter – receiver scheme for structural health monitoring.

As a rule, the exciting signal is a windowed wave packet centered at certain frequency (Rose, 2014, e.g.), and only first recorded reflection is considered. Much longer records at the receiver are used if a time-reversal procedure is expected (Givoli, 2014, e.g.). In an ideal situation, the wave propagates with constant velocity and its propagation from the transmitter to the sensor is straight and can be interrupted only by the investigated defect. However, even if we restrict ourselves to a two-dimensional strip setting, we cannot find the analytical solution for wave propagation in a finite homogeneous strip. The exact analytical approach is feasible only in the case of an infinite strip

as shown by Valeš and Šebková (1976) for a strip with distributed transversal excitation and by Brock (1986) for a suddenly applied transversal point force. Numerical studies dealing with two-dimensional strip problems are more common. One can mention for instance the work (Červ et al., 1993) where the propagation of acoustic emission signal is investigated using the finite element approach.

It should be noted that the strip geometry is closely related to propagation of Lamb waves in thin plates (Lee and Staszewski, 2007; Barouni and Saravanos, 2016), which are widely applied to structural health monitoring problems (Croxford et al., 2007). Modeling of Lamb waves with the desired accuracy, reliability, and efficiency is a valuable part of the methodology, software, and hardware for non-destructive evaluation and structural health monitoring (Willberg et al., 2015). Various numerical methods have been used for their simulations (Lee and Staszewski, 2007; Sundararaman and Adams, 2009; Kluska et al., 2013; Maio et al., 2015; Barouni and Saravanos, 2016, e.g). However, as it is demonstrated in (Leckey et al., 2018), the existing computational packages (ANSYS, COMSOL, ABAQUS) are unable to represent wavefield in laminates adequately. The reason is that the commercial software use one-step time schemes which are not able to prescribe wave propagation in heterogeneous media accurately due to spatial dispersion and transmission/reflection effects on interfaces.

It is, therefore, highly desired to have correct descriptive and computational tools for the prediction of wave propagation in a basic setting. The paper presents the results of the experimental, theoretical, and computational study of the propagation of transient elastic waves from a localized source in a homogeneous aluminium strip. The main goal is to examine and verify the suitability of numerical procedures to represent the transient wavefield observed during the experiment. Section 2 is devoted to the description of the experimental setup and procedure. Governing equations corresponding to linear elasticity are presented in Section 3. Analytical solution and numerical methods are shortly described in Section 4. In Section 5, the comparison of analytical, numerical, and experimental results are presented. Conclusions and discussion are included in the last Section.

2. Experimental setup

Measurements of wave propagation in an elastic strip of finite length were done in the Laboratory of Non-Destructive Testing of the Institute of

Material	Density $\rho\,(\mathrm{kg/m^3})$	Young modulus $E\,(\mathrm{GPa})$	Poisson ratio ν	Longitudinal speed $c_p\,(\mathrm{m/s})$	Shear speed $c_s\,(\mathrm{m/s})$
Al alloy D16-ATV	2770	72	0.333	5401	3126

Table 1: Material properties of the strip under investigation.

Thermomechanics of the Czech Academy of Sciences. The elastic strip was made from a homogeneous isotropic Al alloy D16-ATV. Material parameters that are necessary for wave investigation in such a medium are summarized in Table 1. The value of longitudinal speed c_p corresponds to plane stress conditions.

Dimensions of the strip suspended on thin UHMWPE Dyneema filaments were 399×50×1.35 mm. To induce a loading pulse, the piezoelectric transducer Dakel IDK09 of diameter 6 mm was glued in the middle of the strip from the bottom side (see Fig. 2). The NI PXI test system includes NI PXI 5105 digitizer and NI PXI 5412 generator connected with a custom power pulse amplifier. For the non-contact vibration record, the Polytec vibrometer system was used. The OFV-5000 controller decodes the sensor OVF-505 head's signals in real time. The automated ultrasonic Starmans scanning stage DIO 200 system was applied for the signal inspection. The mentioned

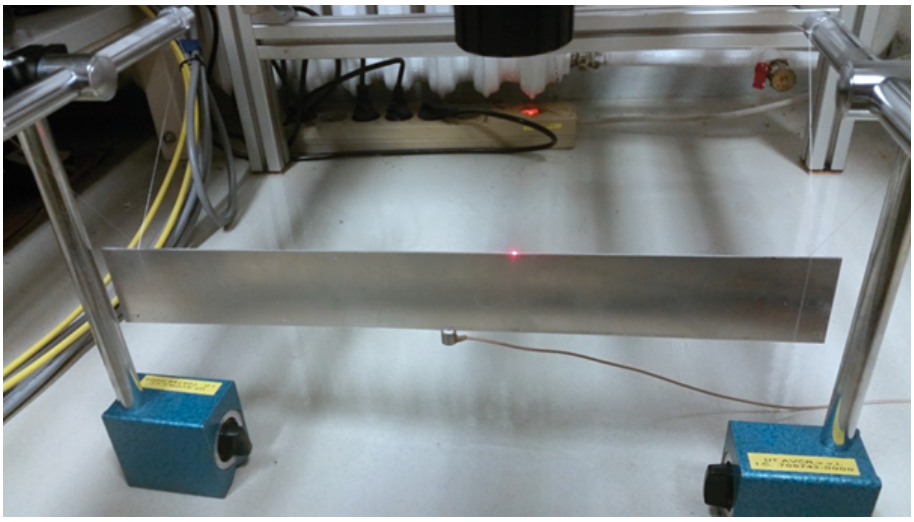

Figure 2: Experimental setup.

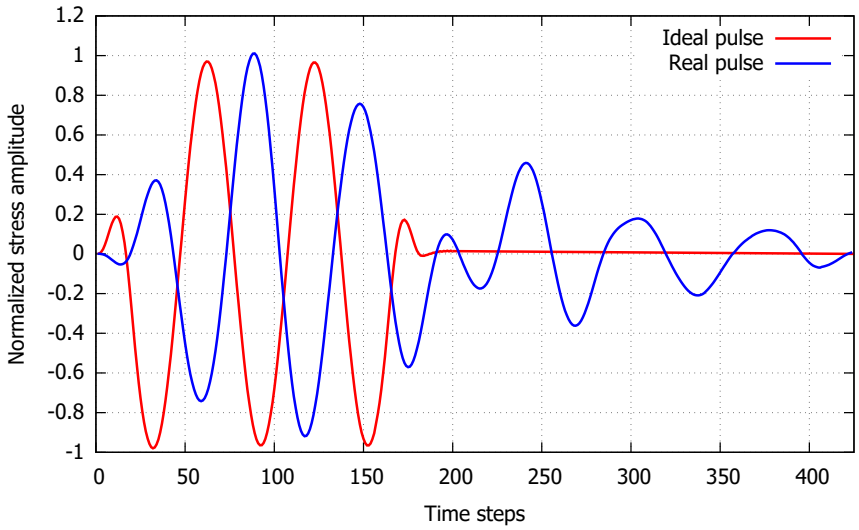

Figure 3: Shape of ideal and real loading pulses.

device enabled the lengthwise scanning along the upper edge at points of a regular grid with the step of 1 mm. The response measured up to 750 μs was represented by 15 000 samples at frequency 20 MHz, i.e. the sampling time step was $\Delta t = 5 \cdot 10^{-8}$ s.

The input signal to the transducer causing the strip loading corresponds to a smooth pulse of duration $t_0 = 9$ μs with maximal amplitude $\sigma_0 = 0.72$ MPa. Its amplitude changes according to cosine train 333 kHz with 0.25 cosine window. This pulse can be expressed as

$$\sigma(t) = \begin{cases} \frac{\sigma_0}{2} \cos\left(\frac{\pi t}{30}\right)\left(1 - \cos\left(\frac{\pi t}{22}\right)\right) & \text{for} \quad t \leq 23\Delta t, \\ \sigma_0 \cos\left(\frac{\pi t}{30}\right) & \text{for} \quad 23\Delta t \leq t \leq 157\Delta t, \\ \frac{\sigma_0}{2} \cos\left(\frac{\pi t}{30}\right)\left(1 - \cos\left(\frac{\pi(180-t)}{22}\right)\right) & \text{for} \quad 157\Delta t \leq t \leq 180\Delta t, \\ 0 & \text{for} \quad t \geq 180\Delta t. \end{cases}$$

The time history of this input signal is shown in Fig. 3 (curve *Ideal pulse*).

The more precise experimental investigation shows that the input signal does not correspond to the real signal exciting the strip (see Fig. 3, curve *Real pulse*). This real pulse is the result of the normal velocity measurement in the center of the transducer surface using a vibrometer. The difference between the ideal pulse (input electric signal into the transducer) and real pulse (corresponding to the normal velocity measured on the transducer sur-

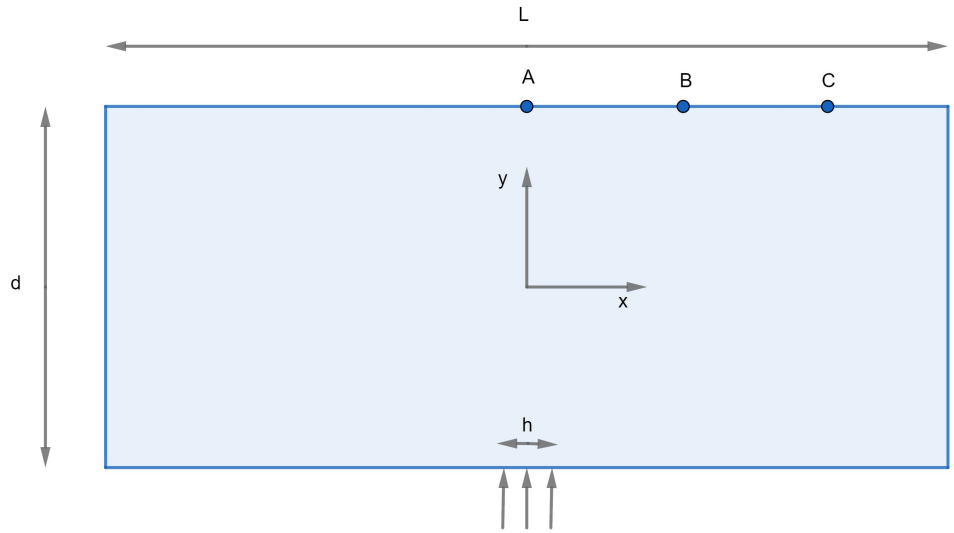

Figure 4: Sketch of the problem.

face) is due to complex wave processes inside the transducer, piezo-electric response, and piezo-electric/mechanical coupling. The shape of the real pulse cannot be represented as a mathematical expression. Moreover, the information about the time history of the normal velocity on the transducer surface can be implemented into the finite element model as a time-varying Dirichlet boundary condition. In parallel, the normal stress loading will be applied via Neumann boundary conditions. In reality, one has to think also about a non-ideal connection between the transducer and the strip under investigation. This effect is neglected both in numerical and analytical solutions of the problem, so an ideal connection between the transducer and the strip is assumed.

3. Model description and mathematical formulation

The problem lies in the investigation of the transient response of an elastic strip to a transversal loading, as mentioned previously. The sketch of the model corresponding to the described measured problem is shown in Fig. 4.

According to the introduced coordinate system and to the experiment description given in Section 2, the stress loading $p(x,t)$ is nonzero only for $y = -d/2$ and $x \in [-h/2, h/2]$. It will be approximated by $p(x,t) =$

$(H(x+h/2)-H(x-h/2))\,\sigma(t)$, where $H(x)$ denotes the Heaviside function in x and $\sigma(t)$ stands for the ideal or real pulse from Fig. 3. The problem was solved as the symmetric one and the evaluation of vertical velocity component up to time $t_{max} = 750$ μs was primarily made at points A, B, and C for comparison with experimental data. The position of these points is shown in Fig. 4 and the distance between them is 13.5 mm each.

The problem is considered in the framework of small strain elasticity theory. For thin strip, we use the plane stress approximation suggesting that stress normal to the strip plane and appropriate shear stresses can be neglected, i.e.,

$$\sigma_{i3} = 0, \quad i = 1, 2, 3. \tag{1}$$

The governing equations of homogeneous linear isotropic elasticity in the absence of body forces specialized to plane stress conditions have the form

$$\rho\frac{\partial v_1}{\partial t} = \frac{\partial \sigma_{11}}{\partial x} + \frac{\partial \sigma_{12}}{\partial y}, \tag{2}$$

$$\rho\frac{\partial v_2}{\partial t} = \frac{\partial \sigma_{21}}{\partial x} + \frac{\partial \sigma_{22}}{\partial y}, \tag{3}$$

where t is time, v_i are the components of the velocity vector, σ_{ij} is the Cauchy stress tensor and ρ is the density.

Accordingly, compatibility conditions for strains are represented as

$$\frac{\partial \varepsilon_{11}}{\partial t} = \frac{\partial v_1}{\partial x}, \tag{4}$$

$$\frac{\partial \varepsilon_{12}}{\partial t} = \frac{1}{2}\left(\frac{\partial v_1}{\partial y} + \frac{\partial v_2}{\partial x}\right), \tag{5}$$

$$\frac{\partial \varepsilon_{22}}{\partial t} = \frac{\partial v_2}{\partial y}. \tag{6}$$

The Hooke law defining the stress-strain relation is modified as follows:

$$\sigma_{11} = (\overline{\lambda} + 2\mu)\varepsilon_{11} + \overline{\lambda}\varepsilon_{22}, \tag{7}$$

$$\sigma_{12} = \sigma_{21} = 2\mu\varepsilon_{12}, \tag{8}$$

$$\sigma_{22} = (\overline{\lambda} + 2\mu)\varepsilon_{22} + \overline{\lambda}\varepsilon_{11}, \tag{9}$$

where $\overline{\lambda} = 2\mu\lambda/(\lambda+2\mu)$ and λ and μ are the Lamé coefficients. Compatibility conditions (4)–(6) allow to eliminate strains in time derivatives of stress-strain relations

$$\frac{\partial \sigma_{11}}{\partial t} = (\overline{\lambda} + 2\mu)\frac{\partial v_1}{\partial x} + \overline{\lambda}\frac{\partial v_2}{\partial y}, \tag{10}$$

$$\frac{\partial \sigma_{22}}{\partial t} = \overline{\lambda}\frac{\partial v_1}{\partial x} + (\overline{\lambda} + 2\mu)\frac{\partial v_2}{\partial y}, \tag{11}$$

$$\frac{\partial \sigma_{12}}{\partial t} = \frac{\partial \sigma_{21}}{\partial t} = \mu\left(\frac{\partial v_1}{\partial y} + \frac{\partial v_2}{\partial x}\right). \tag{12}$$

Together with the balance of linear momentum (2)–(3), latter equations form the system of equations, which is convenient for the solution.

4. Solution methods

4.1. Analytical solution

As mentioned in Section 1, there exists the analytical solution of an infinite elastic strip problem derived by (Valeš and Šebková, 1976). In our study, we generalized this solution to an arbitrary type of external loading and use the evaluation procedure similar to that presented in the work (Adámek and Valeš, 2015). This two-step procedure involves the inverse Laplace transform and the evaluation of Fourier integral. The latter one issue is addressed by classical Simpson's rule with a regular integration grid while the first one is resolved by the application of an algorithm based on fast Fourier transform and Wynn's epsilon accelerator. The precision and the stability of this procedure is discussed in detail in (Adámek et al., 2017).

4.2. Finite volume computations

Among finite volume methods, the most suitable for our purpose is the wave propagation algorithm (LeVeque, 2002). Its two-dimensional implementation is applied for the simulation of wave propagation in the finite elastic strip. The thermodynamically consistent version of the algorithm (Berezovski et al., 2008) is employed with values of the Courant number close to unity. The applied method is second-order accurate on smooth solutions (Bale et al., 2003). Boundary conditions are imposed using ghost cells following (LeVeque, 2002).

4.3. Finite element computations

In the finite element computations based on an in-house code, we use the displacement formulation with linear shape functions (Hughes, 2000), which are preferred in explicit time integration with the lumped mass matrix. The central difference method for direct time integration is employed, therefore the stability limit according to the Courant–Friedrichs–Lewy condition should be satisfied, see (Courant et al., 1928). For evaluation of the stiffness matrix, the one-Gauss point integration with the hourglass stabilization (Belytschko and Bachrach, 1986) is utilized. For the maximum frequency contained in the loading pulse, the length of the finite element edge is set to 0.25 mm due to the spatial dispersion of the finite element method (Kolman et al., 2016). The time step size corresponds to the Courant number $Co = 0.97$.

5. Infinite strip

To validate the accuracy of both numerical methods, it is instructive to start with the problem of an infinite strip for which the analytical solution exists. According to the experimental setup, the time step $\Delta t = 5 \cdot 10^{-8} s$ and the ideal pulse of duration $t_0 = 180\,\Delta t = 9$ μs are used at first. Space step for explicit schemes corresponds to the Courant number $Co = 1$ determined by the maximum of longitudinal velocity in material. In the case of Al alloy D16-ATV, the longitudinal wave velocity is equal to 5401 m/s which means that $\Delta x = c_p \cdot \Delta t = 0.27$ mm. It follows then that the strip width $d = 50$ mm $= 185\,\Delta x$ and the loading length $h = 6$ mm $= 22\,\Delta x$.

Using these values, the computation of wave propagation in the strip under ideal loading via the normal stress shown in Fig. 3 was performed analytically and by finite volume and finite element methods. Results of numerical simulations and analytical solution are compared at all three points. The comparison at point A that corresponds to the middle of the strip is presented in Fig. 5. As one can see, the results of simulations by finite volume and finite element methods are almost coinciding with the analytical solution up to 2000 time steps (100 μs), i.e., at early stages of the signal propagation. Similar results have been obtained also for points B and C. After 2000 time steps, the results start to diverge due to the influence of lateral vertical boundaries of the strip used in numerical models. Based on this comparison, we can conclude that the chosen finite element and finite volume methods are suitable for the elastic wave propagation problem in the strip.

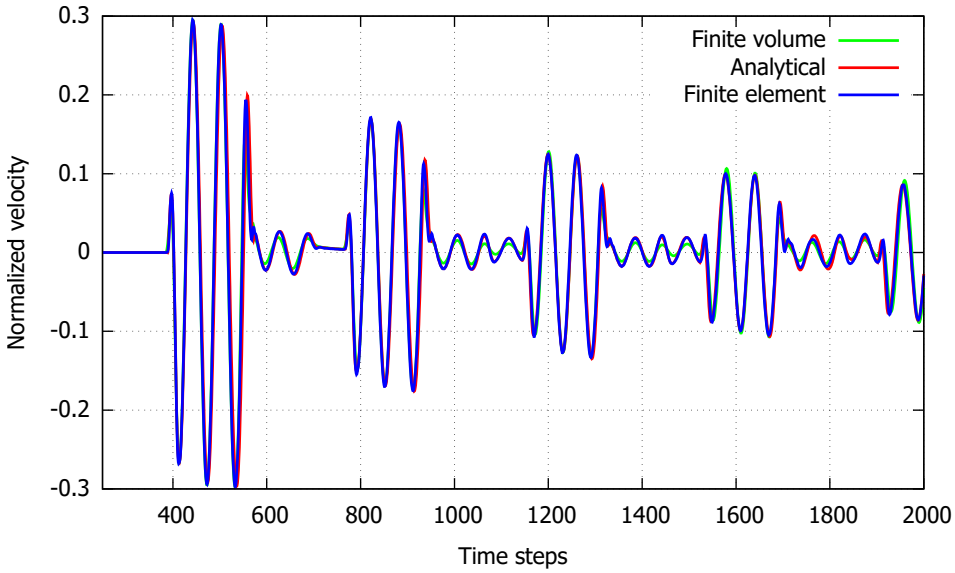

Figure 5: The response to the ideal pulse: analytical solution vs numerical simulations.

The same coincidence between the analytical and numerical solutions was achieved also for the real pulse excitation. Making such verification of applied approaches, the obtained results can be compared with the measured strip response to the real pulse. This comparison is presented in Fig. 6 - 8 for all three studied points. Due to the mentioned coincidence between analytical and numerical solutions, only analytical and experimental results are shown.

It is seen that the very good agreement with the measured data occurs for the first 1000 time steps (i.e. up to time 50 μs), especially at point B (see Fig. 7). Considering the time history for the vertical velocity at point C (Fig. 8), we cannot say that the agreement with the experiment is as good as at the previous points even for the short time simulations. Also for longer times, the dispersion properties of the real strip and the real structure of the strip material make the differences between both responses more significant at all three points.

The application of the Dirichlet boundary condition for the normal velocity is also checked in the finite element simulations. The results of the time history of the normal velocity at the point B are depicted in Fig. 9 as an example. One can see that the results for Dirichlet and Neumann boundary

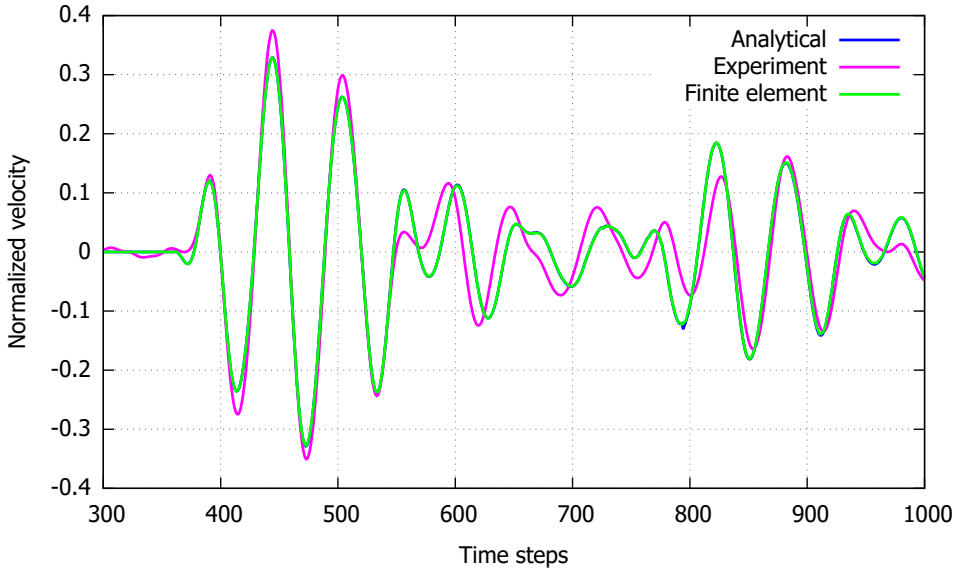

Figure 6: The response to the real pulse at point A: analytical and numerical solution vs experimental data.

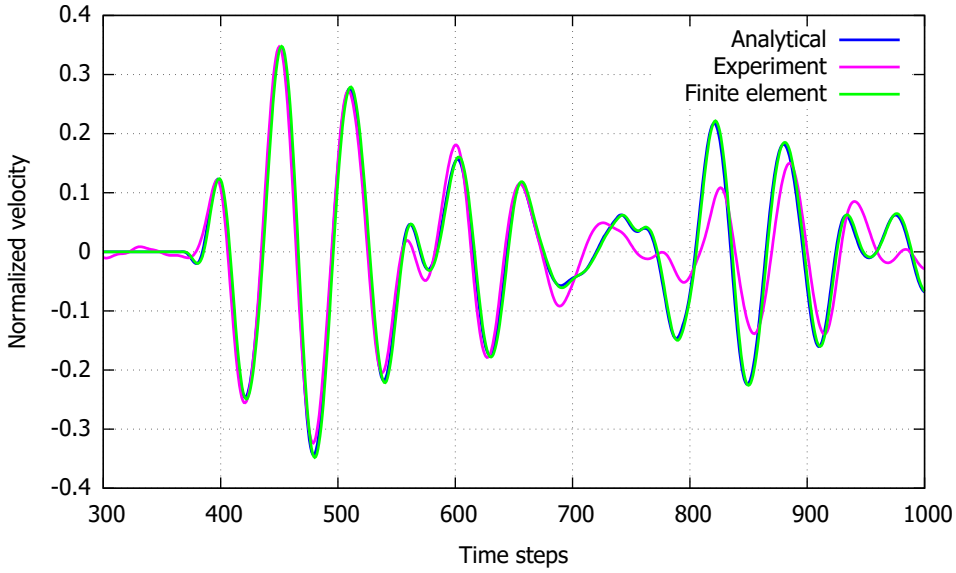

Figure 7: The response to the real pulse at point B: analytical and numerical solution vs experimental data.

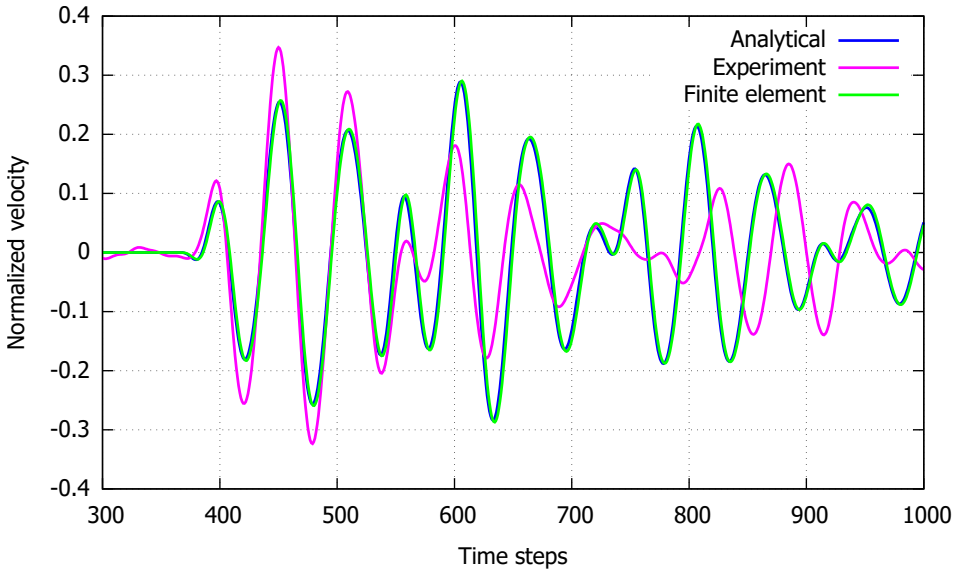

Figure 8: The response to the real pulse at point C: analytical and numerical solution vs experimental data.

conditions are very close to each other. So it can be said that both types of boundary conditions can be used for correct representation of transducer loading.

Having the verified analytical and numerical models for short time response of the real strip, one can use these models to visualize the wavefield the consequences of which have been measured at the strip edge. For this purpose, the snapshots of the mean velocity $\sqrt{v_1^2 + v_2^2}$ at various time instants obtained by the analytical solution are shown in Fig. 10. This picture demonstrates how the wave field is varied due to reflections from upper and bottom boundaries and internal interferences. A clear separation between the longitudinal wave and the pattern of remaining wave interference is observed.

6. Finite strip

In the case of finite strip, we need to take into account the reflections from the lateral vertical boundaries. It requires computations for a longer time. The comparison of experimental data with analytical solution and numerical results obtained by the finite element method is shown in Fig. 11. The results of finite volume simulation are not presented because they

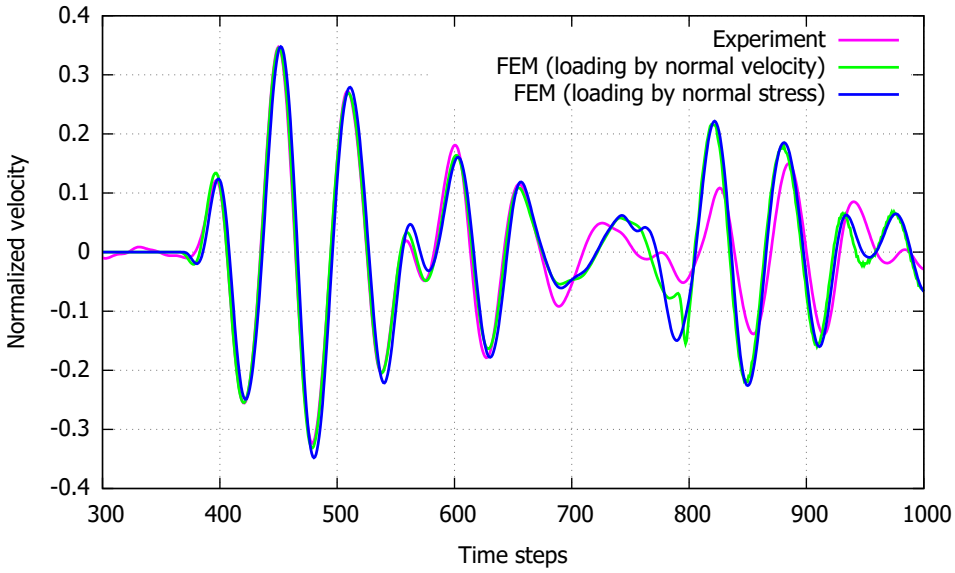

Figure 9: The response to the real pulse at point B obtained by the stress and velocity loading.

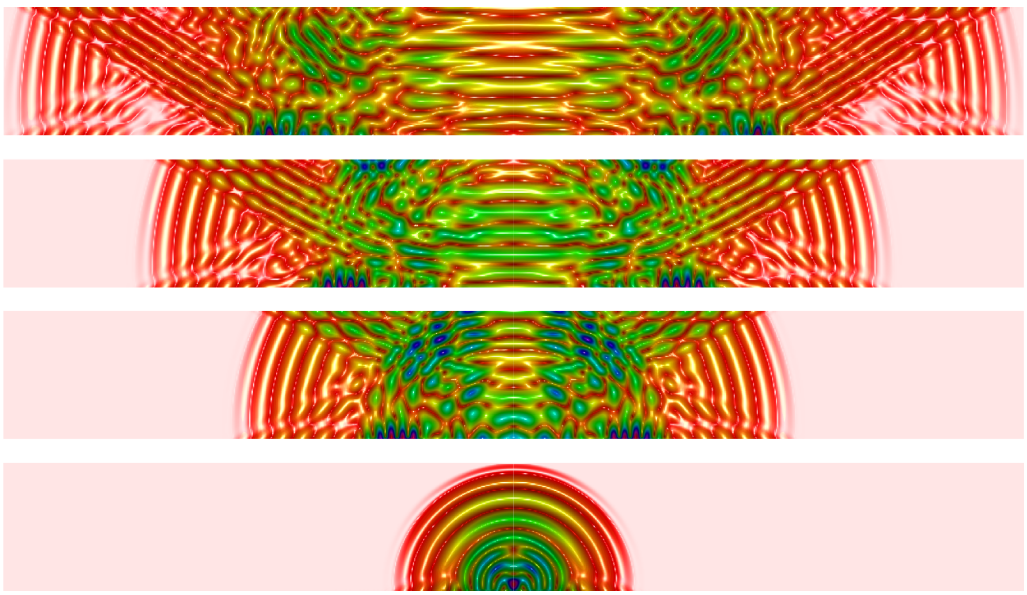

Figure 10: Distribution of the mean velocity $\sqrt{v_1^2 + v_2^2}$ inside the strip. Snapshots of the analytical solution for $t = \{186\Delta t, 420\Delta t, 561\Delta t, 753\Delta t\}$.

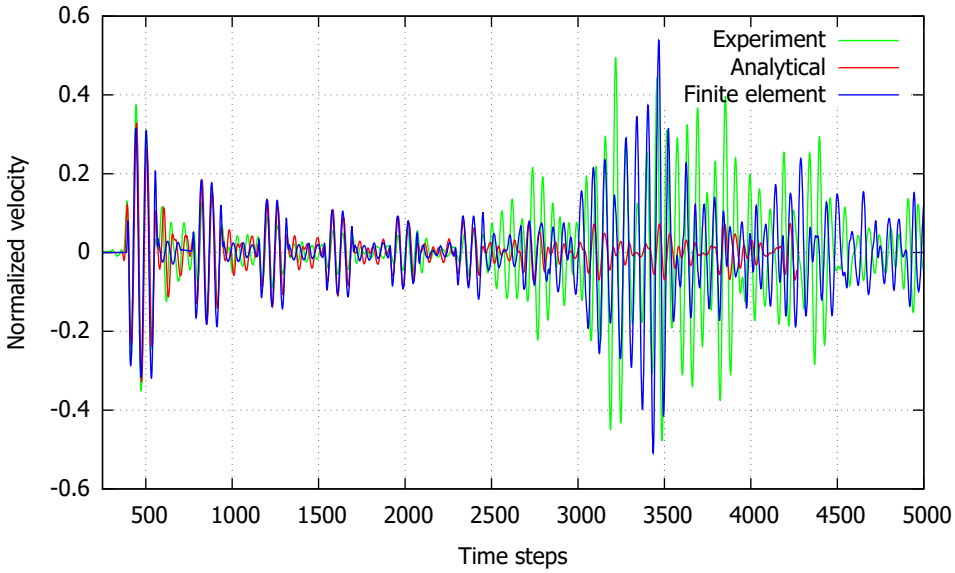

Figure 11: Measured response vs analytical solution and finite element computation for longer time.

are nearly identical to analytical ones up to about 2000 time steps and for longer times they do not conserve the total energy of the signal. It is clear from Fig. 11 that all results coincide quite well up to about 2500 time steps. After this time instant, the analytical solution does not represent the real response due to the absence of lateral strip boundaries influence. The results of finite element computations take the reflections from lateral boundaries into account, but uncertainties in experimental setup prevent the detailed coincidence.

In an attempt to improve the agreement between numerical simulations and experimental data, the 3D computation of the problem was performed using the in-house finite element code. Unfortunately, the results of 3D calculation differ from those in 2D only slightly, as it can be clearly seen in Fig. 12. From one side, it confirms that the applied plane stress approximation is applicable for the considered problem. From another side, it does not assure that 3D computing will improve the results of numerical modeling significantly.

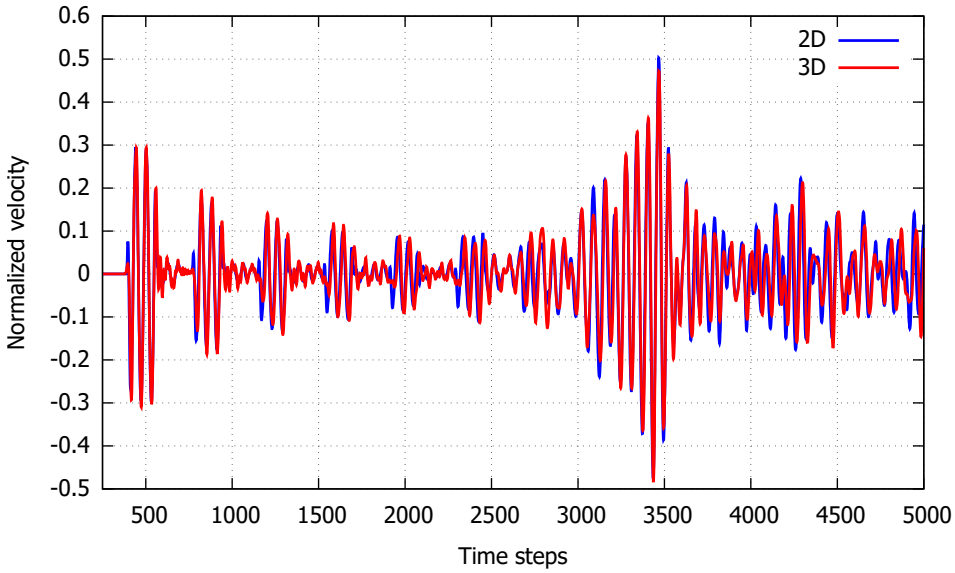

Figure 12: Comparison of results for finite element 2D and 3D simulation.

7. Conclusions

Experimental measurements and numerical simulations were performed to examine the accuracy of the plane stress approximation in the description of elastic waves in a finite strip. The comparison of experimental data with the analytical solution and numerical simulations demonstrates the ability of standard numerical methods to reproduce the signal propagation in a homogeneous strip only for short time computations. The obtained results confirm the suitability of existing nondestructive evaluation methods and pose certain questions concerning the time-reversal technique using long-time computing.

Acknowledgments

The work was supported by the grant projects with No. 19-04956S of the Czech Science Foundation (CSF) within institutional support RVO:61388998, by the Centre of Excellence for Nonlinear Dynamic Behaviour of Advanced Materials in Engineering CZ.02.1.01/0.0/0.0/15_003/0000493 (Excellent Research Teams) in the framework of Operational Programme Research, Development and Education and by the project LO1506 of the Czech Ministry of

Education, Youth and Sports under the program NPU I. A.B. acknowledges the support by the Estonian Research Council under Institutional Research Funding IUT33-24.

References

Adámek, V., Valeš, F., 2015. Analytical solution for transient response of an infinite viscoelastic strip. Journal of Vibration Engineering and Technologies 3, 699–710.

Adámek, V., Valeš, F., Červ, J., 2017. Numerical Laplace inversion in problems of elastodynamics: Comparison of four algorithms. Advances in Engineering Software 113, 120–129.

Bale, D.S., LeVeque, R.J., Mitran, S., Rossmanith, J.A., 2003. A wave propagation method for conservation laws and balance laws with spatially varying flux functions. SIAM Journal on Scientific Computing 24, 955–978.

Barouni, A.K., Saravanos, D.A., 2016. A layerwise semi-analytical method for modeling guided wave propagation in laminated and sandwich composite strips with induced surface excitation. Aerospace Science and Technology 51, 118–141.

Belytschko, T., Bachrach, W.E., 1986. Efficient implementation of quadrilaterals with high coarse-mesh accuracy. Computer Methods in Applied Mechanics and Engineering 54, 279–301.

Berezovski, A., Engelbrecht, J., Maugin, G.A., 2008. Numerical Simulation of Waves and Fronts in Inhomogeneous Solids. World Scientific Singapore.

Brock, L., 1986. The transient field under a point force acting on an infinite strip. Journal of Applied Mechanics 53, 321–325.

Courant, R., Friedrichs, K., Lewy, H., 1928. Über die partiellen ifferenzengleichungen der mathematischen Physik. Mathematische Annalen 100, 32–74.

Croxford, A., Wilcox, P., Drinkwater, B., Konstantinidis, G., 2007. Strategies for guided-wave structural health monitoring. Proceedings of the Royal Society A: Mathematical, Physical and Engineering Sciences 463, 2961–2981.

Givoli, D., 2014. Time reversal as a computational tool in acoustics and elastodynamics. Journal of Computational Acoustics 22, 1430001.

Hughes, T.J.R., 2000. The Finite Element Method: Linear Static and Dynamic Finite Element Analysis. Dover Publication.

Kluska, P., Staszewski, W., Leamy, M., Uhl, T., 2013. Cellular automata for Lamb wave propagation modelling in smart structures. Smart Materials and Structures 22, 085022.

Kolman, R., Plešek, J., Červ, J., Okrouhlík, M., Pařík, P., 2016. Temporal-spatial dispersion and stability analysis of finite element method in explicit elastodynamics. International Journal for Numerical Methods in Engineering 106, 113–128.

Leckey, C.A., Wheeler, K.R., Hafiychuk, V.N., Hafiychuk, H., Timuçin, D.A., 2018. Simulation of guided-wave ultrasound propagation in composite laminates: Benchmark comparisons of numerical codes and experiment. Ultrasonics 84, 187–200.

Lee, B., Staszewski, W., 2007. Lamb wave propagation modelling for damage detection: I. two-dimensional analysis. Smart Materials and Structures 16, 249.

LeVeque, R.J., 2002. Finite Volume Methods for Hyperbolic Problems. volume 31. Cambridge University Press.

Maio, L., Memmolo, V., Ricci, F., Boffa, N., Monaco, E., Pecora, R., 2015. Ultrasonic wave propagation in composite laminates by numerical simulation. Composite Structures 121, 64–74.

Rose, J.L., 2014. Ultrasonic Guided Waves in Solid Media. Cambridge University Press.

Sundararaman, S., Adams, D.E., 2009. Accuracy and convergence using a local interaction simulation approach in one, two, and three dimensions. Journal of Applied Mechanics 76, 031008.

Valeš, F., Šebková, H., 1976. The state of stress in non-stationary loaded thin belt. Acta Technica ČSAV 4, 439–458.

Červ, J., Landa, M., Převorovský, Z., 1993. Numerical modelling of acoustic emission signal propagation in a strip. Applied Mechanics Reviews 49(4-6), 6A182.

Willberg, C., Duczek, S., Vivar-Perez, J., Ahmad, Z., 2015. Simulation methods for guided wave-based structural health monitoring: A review. Applied Mechanics Reviews 67, 010803.